Moment-based Analysis of Mechanical Effects on Trench-Hall Devices

Stefano Taschini, Jan G. Korvink* and Henry Baltes

Physical Electronics Laboratory, ETH Zurich, taschini@ieee.org
ETH Hönggerberg HPT-H6, CH-8093 Zürich, Switzerland
*Institute for Microsystem Technology, University of Freiburg, Germany

ABSTRACT

This paper presents a novel method for the assessment of mechanical effects on trench-Hall devices based on a moment expansion combined with two-dimensional finite-element discretization. Analogously to plate theories, a truncated moment expansion of the equations in the transverse coordinate is used to approximate the three dimensional problem. The resulting limited set of two-dimensional problems is discretized by means of finite-elements. The parametrization of the procedure lends itself to the optimization of the device geometry, therefore representing a valuable tool for the designer.

Keywords: Hall effect, finite-element method, moment expansion, mechanical stress.

1. INTRODUCTION

In integrated Hall sensors, besides stress-induced device offset due to the piezoresistance effect, a stress dependence of the magnetic sensitivity due to the modulation of the Hall coefficient, the so-called piezo-Hall effect, affects the quality of the device. Trench-Hall devices [1] have been devised to address the cross-sensitivity caused by the poor carrier confinement in conventional vertical Hall devices. At the same time, its compatibility with CMOS fabrication technology allows the integration with read-out and conditioning circuitry, thus enabling cost-effective miniaturization and high-volume production. Unfortunately, during the fabrication, and in particular during the high-temperature steps in the pre-CMOS-processing, the overlying of dielectric and conducting films with different thermomechanical properties introduces sources of mechanical stress. Important steps have been carried out towards the minimization of the offset [2], but there is still much to investigate in the presence of magnetic field.

The high aspect ratio of the device introduces problems of accuracy and resource consumption into the numerical simulation. These problems, mainly due to the large number of three-dimensional elements required to provide good interpolation properties, can be circumvented by using the same approach found in structural mechanics with plate theories. Plate theories postulate a low-degree polynomial dependence of the displacement with respect to the transverse coordinate, eventually leading to a moment expansion of the momentum balance equation.

2. PIEZO-HALL-DRIFT TRANSPORT

Electronic transport in a n-type semiconductor is dominated by ohmic drift with a correction due to the magnetic induction in the form of

$$\boldsymbol{J} - \mu^* \boldsymbol{B} \times \boldsymbol{J} = \sigma \boldsymbol{E}\,, \tag{1}$$

where μ^* is the Hall-mobility [3]. Under mechanical stress, the two scalar coefficients μ^* and σ in equation (1) are replaced by two tensors $\boldsymbol{\mu}^*$ and $\boldsymbol{\sigma}$ with a local dependence on the stress field. For not too large stress levels, a linearized dependence is justified. The dependence of the conductivity on the stress tensor $\boldsymbol{T}$ is formulated in terms of the fourth-order tensor $\boldsymbol{\pi}$ of the piezoresistance coefficients [4]:

$$\boldsymbol{\sigma} = \sigma(\boldsymbol{I}_3 - \boldsymbol{\pi} : \boldsymbol{T})\,. \tag{2}$$

In equation (2), $\boldsymbol{I}_3$ denotes the three-dimensional identity matrix; the double contraction $\boldsymbol{\pi} : \boldsymbol{T}$ is defined in terms of the cartesian coordinates of the tensors as

$$(\boldsymbol{\pi} : \boldsymbol{T})_{ij} = \sum_{k=1}^{3} \sum_{l=1}^{3} \pi_{ijkl} T_{kl}\,. \tag{3}$$

Similarly, the piezo-Hall coefficients [5] form the fourth-order tensor $\boldsymbol{P}$ relating the Hall mobility to the stress:

$$\boldsymbol{\mu}^* = \mu^*(\boldsymbol{I}_3 + \boldsymbol{P} : \boldsymbol{\sigma})\,. \tag{4}$$

By introducing the dimensionless effective magnetic induction $\boldsymbol{B}^* = \boldsymbol{\mu}^* \cdot \boldsymbol{B}$, equation (1) becomes

$$\boldsymbol{J} - \boldsymbol{B}^* \times \boldsymbol{J} = \boldsymbol{\sigma} \cdot \boldsymbol{E}\,. \tag{5}$$

Solving equation (5) for the current density, yields the anisotropic linearity relation $\boldsymbol{J} = \boldsymbol{\sigma}^* \cdot \boldsymbol{E}$ with the tensor

$$\boldsymbol{\sigma}^* = \frac{1}{1 + (\boldsymbol{B}^*)^2}[\boldsymbol{I}_3 + \boldsymbol{B}^* \times \ + \boldsymbol{B}^* \otimes \boldsymbol{B}^*] \cdot \boldsymbol{\sigma} \tag{6}$$

as the effective conductivity. In equation (6), $\boldsymbol{B}^* \times$ denotes the tensor that contracted with an arbitrary vector $\boldsymbol{u}$ yields the cross product $\boldsymbol{B}^* \times \boldsymbol{u}$; the symbol $\otimes$ denotes the tensor product. Equation (6) is verified immediately by inserting Ohm's law $\boldsymbol{J} = \boldsymbol{\sigma}^* \cdot \boldsymbol{E}$ into the left-hand side of equation (5).

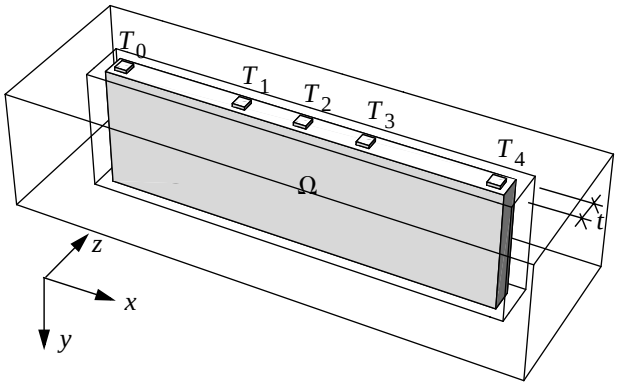

FIGURE 1. Geometry of a trench-Hall device with surface contacts [1]. The contacts T_0 and T_4 are at identical potential. The origin of the reference system is set at the center of the contact T_2.

In order to proceed with the discretization, a variational formulation for the transport equation is necessary. Stemming from the continuity equation for the current is the variational equation

$$(\boldsymbol{J}\cdot\boldsymbol{n},\delta\psi)_{\partial\Omega}-(\boldsymbol{J},\nabla\delta\psi)_{\Omega}=(\nabla\boldsymbol{J},\delta\psi)_{\Omega}=0\,, \tag{7}$$

where $\delta\psi$ is an arbitrary variation of the potential satisfying the essential boundary conditions. In equation (7), the forms $(\bullet,\bullet)_{\Omega}$ and $(\bullet,\bullet)_{\partial\Omega}$ denote the integral product on the domain Ω and its boundary $\partial\Omega$, respectively. Since $\boldsymbol{J}=-\boldsymbol{\sigma}^*\cdot\nabla\psi$, equation (7) is recast in terms of the electrostatic potential as

$$(\boldsymbol{\sigma}^*\cdot\nabla\psi,\nabla\delta\psi)_{\Omega}+(\boldsymbol{J}\cdot\boldsymbol{n},\delta\psi)_{\partial\Omega}=0\,. \tag{8}$$

A three-dimensional finite-element approximation of equation (8) on a plate like that of figure 1 is demanding in terms of resources per accuracy, in general leading to poor results. The following section focuses on an alternative approach for the discretization of equation (8) that takes advantage of the particular characteristics of the plate geometry.

3. MOMENT EXPANSION

In a geometry like that of figure 1, it is convenient to separate the vector and tensor components parallel and perpendicular to the plate. In terms of the cartesian components relative to the reference system of figure 1, Ohm's law reads

$$\begin{bmatrix}J_x\\J_y\\J_z\end{bmatrix}=\begin{bmatrix}\sigma_{xx}&\sigma_{xy}&\sigma_{xz}\\\sigma_{yx}&\sigma_{yy}&\sigma_{yz}\\\sigma_{zx}&\sigma_{zy}&\sigma_{zz}\end{bmatrix}\begin{bmatrix}E_x\\E_y\\E_z\end{bmatrix}, \tag{9}$$

where the asterisk of the effective conductivity is omitted. The strong carrier confinement imposed by the trench around the Hall-plate justifies the assumption that the conduction takes place only parallel to the plate, i.e. that the perpendicular component of the current density J_z is identically null. In this case, Schur's complement of σ_{zz} in the conductivity tensor allows the reduction of equation (9) to the in-plane components only:

$$\begin{bmatrix}J_x\\J_y\end{bmatrix}=\left\{\begin{bmatrix}\sigma_{xx}&\sigma_{xy}\\\sigma_{yx}&\sigma_{yy}\end{bmatrix}-\frac{1}{\sigma_{zz}}\begin{bmatrix}\sigma_{xz}\\\sigma_{yz}\end{bmatrix}\begin{bmatrix}\sigma_{zx}&\sigma_{zy}\end{bmatrix}\right\}\begin{bmatrix}E_x\\E_y\end{bmatrix}. \tag{10}$$

It is therefore possible to give the interpretation of the symbols $\boldsymbol{J}$, $\boldsymbol{\sigma}^*$ and $\boldsymbol{E}$ according to equation (10). The plate Ω with thickness t can be thought of as the cartesian product of its middle plane ω, on which the x and y axes are located, and the interval $[-t/2,\,t/2]$ along the z axis. Since $J_z=0$, the variational equation (8) becomes

$$\int_{-t/2}^{t/2}\{(\boldsymbol{\sigma}^*\cdot\nabla\psi,\nabla\delta\psi)_{\omega}+(\boldsymbol{J}\cdot\boldsymbol{n},\delta\psi)_{\partial\omega}\}\,\mathrm{d}z=0\,. \tag{11}$$

The truncated power-series expansion of the potential relative to the transverse coordinate z,

$$\psi(x,y,z)=\sum_{i=0}^{n}\psi_i(x,y)z^i\,, \tag{12}$$

and, consistently, of its variation

$$\delta\psi(x,y,z)=\sum_{i=0}^{n}\delta\psi_i(x,y)z^i\,, \tag{13}$$

are inserted into the variational equation (11), so as to obtain

$$\sum_{i,\,j}(m_{i+j}[\boldsymbol{\sigma}^*]\cdot\nabla\psi_i,\nabla\delta\psi_j)_{\omega}+\sum_i(m_i[\boldsymbol{J}]\cdot\boldsymbol{n},\delta\psi_i)_{\partial\omega}=0 \tag{14}$$

In equation (14), $m_{i+j}[\boldsymbol{\sigma}^*]$ and $m_i[\boldsymbol{J}]$ are the moments of of the conductivity and terminal current density. For a generic tensor field $\boldsymbol{u}$, the moment of order k in z is defined as

$$m_k[\boldsymbol{u}]=\int_{-t/2}^{t/2}z^k\boldsymbol{u}\,\mathrm{d}z\,,$$

which vanishes for odd values of k under symmetry conditions around the middle plane. If $\boldsymbol{u}$ is uniform across the plate, then, for even values of k,

$$m_k[\boldsymbol{u}]=\int_{-t/2}^{t/2}z^k\boldsymbol{u}\,\mathrm{d}z=\frac{2}{1+k}\left(\frac{t}{2}\right)^{k+1}\boldsymbol{u}\,. \tag{15}$$

For the case $n=2$, the resulting equations are

$$(m_0[\boldsymbol{\sigma}^*]\cdot\nabla\psi_0+m_2[\boldsymbol{\sigma}^*]\cdot\nabla\psi_2,\nabla\delta\psi_0)_{\omega}+(m_0[\boldsymbol{J}]\cdot\boldsymbol{n},\delta\psi_0)_{\partial\omega}=0 \tag{16}$$

$$(m_2[\boldsymbol{\sigma}^*]\cdot\nabla\psi_1,\nabla\delta\psi_1)_{\omega}=0 \tag{17}$$

$$(m_2[\boldsymbol{\sigma}^*]\cdot\nabla\psi_0+m_4[\boldsymbol{\sigma}^*]\cdot\nabla\psi_2,\nabla\delta\psi_2)_{\omega}+(m_2[\boldsymbol{J}]\cdot\boldsymbol{n},\delta\psi_2)_{\partial\omega}=0 \tag{18}$$

By virtue of the absence of source terms in equation (17), if the boundary conditions for ψ are symmetric with respect to the middle plane, then ψ_1 is identically zero. The coupled system (16,18) in (ψ_0, ψ_2) is then discretized by means of two-dimensional finite-elements.

4. SIMULATION

The mechanical boundary conditions for the plate suggest that the stress analysis can be conducted on a cross section perpendicular to the z axis (figure 2).

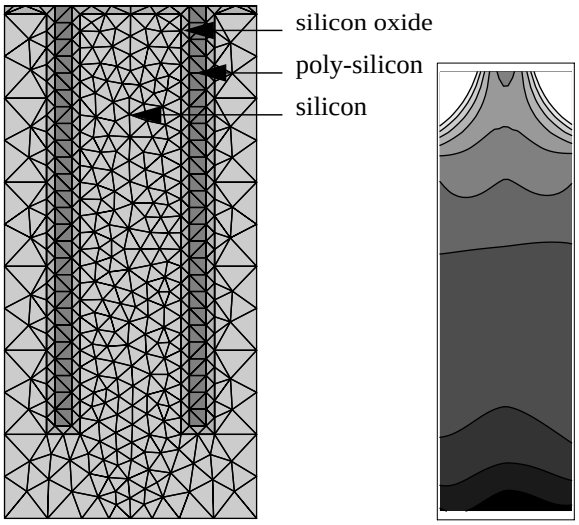

FIGURE 2. On the left, cross section of the trench-Hall plate. On the right, contour plot of the isotropic component of the stress tensor (cf. figure 3). The slight asymmetry is due to the asymmetry of the mesh. The trench is 8μm deep and 0.8μm wide.

Using a thermomechanical finite-element simulator [6], it is possible to estimate the stress state of the structure by following the temperature trend during the fabrication steps, and then letting the temperature drop to working conditions, so as to reproduce the stress induced by the overlying of the oxide and poly-crystalline silicon layers. This method easily introduces crude approximations that weaken the reliability for the results. On the other hand, the purpose of this method is to gain insight in the stress profile more than determining precise values for the stress, whose magnitude is anyway affected by many other circumstances.

The isotropic and shear components of the stress show similar profile, as shown in figure 3. By virtue of equations (2–6) the stress profile is combined with the magnetic induction $\boldsymbol{B}$ to obtain the effective conductivity $\boldsymbol{\sigma}^*$. Following the expansion outlined in section 3, $\boldsymbol{\sigma}^*$ is replaced by the Schur's complement of its component perpendicular to the plate.

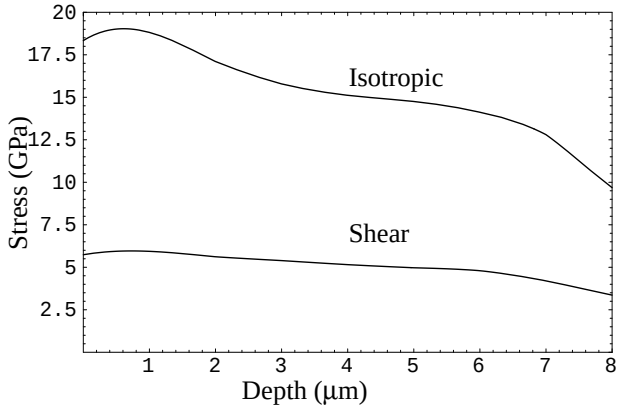

FIGURE 3. The plot of the isotropic and shear components of the stress at the center of the plate against the depth.

The generalized electroresistive problem can be solved using finite elements as shown in figure 4 for a magnetic induction perpendicular to the plate. The simulation refers to the configuration of figure 1 with T_2 as the driving terminal, T_0 and T_4 at ground, T_1 and T_3 as the sensing terminals. The length of the plate is 40.8μm and the contact size is 0.8μm. The centers of the terminals $T_0 - T_5$ are located at -19.6μm, -6.8μm, 0, 6.8μm, 19.6μm, respectively. By parametrizing any of these values it is possible to conduct searches in the parameter space to optimize the device with respect to a given functional. Alternatively, the orientation of the magnetic induction can be taken as a parameter, as shown in figure 5.

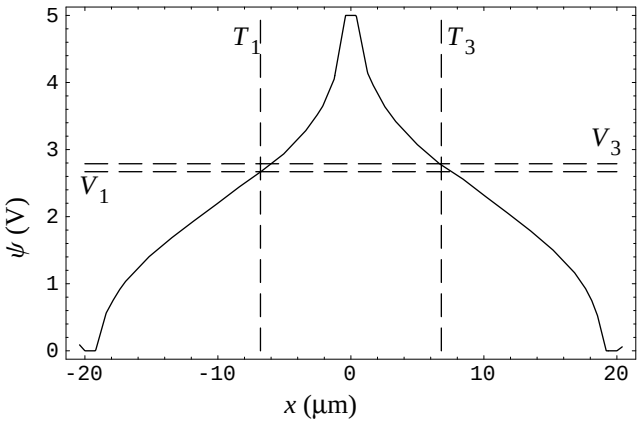

FIGURE 4. The potential ψ at the surface of the plate. The Hall voltage is given by the difference $V_3 - V_1$ of the potentials of the terminals T_3 and T_1.

5. CONCLUSIONS

The moment expansion of the piezo-Hall-drift transport equation presented in this paper represents an effective numerical scheme for the analysis of the mechanical stress

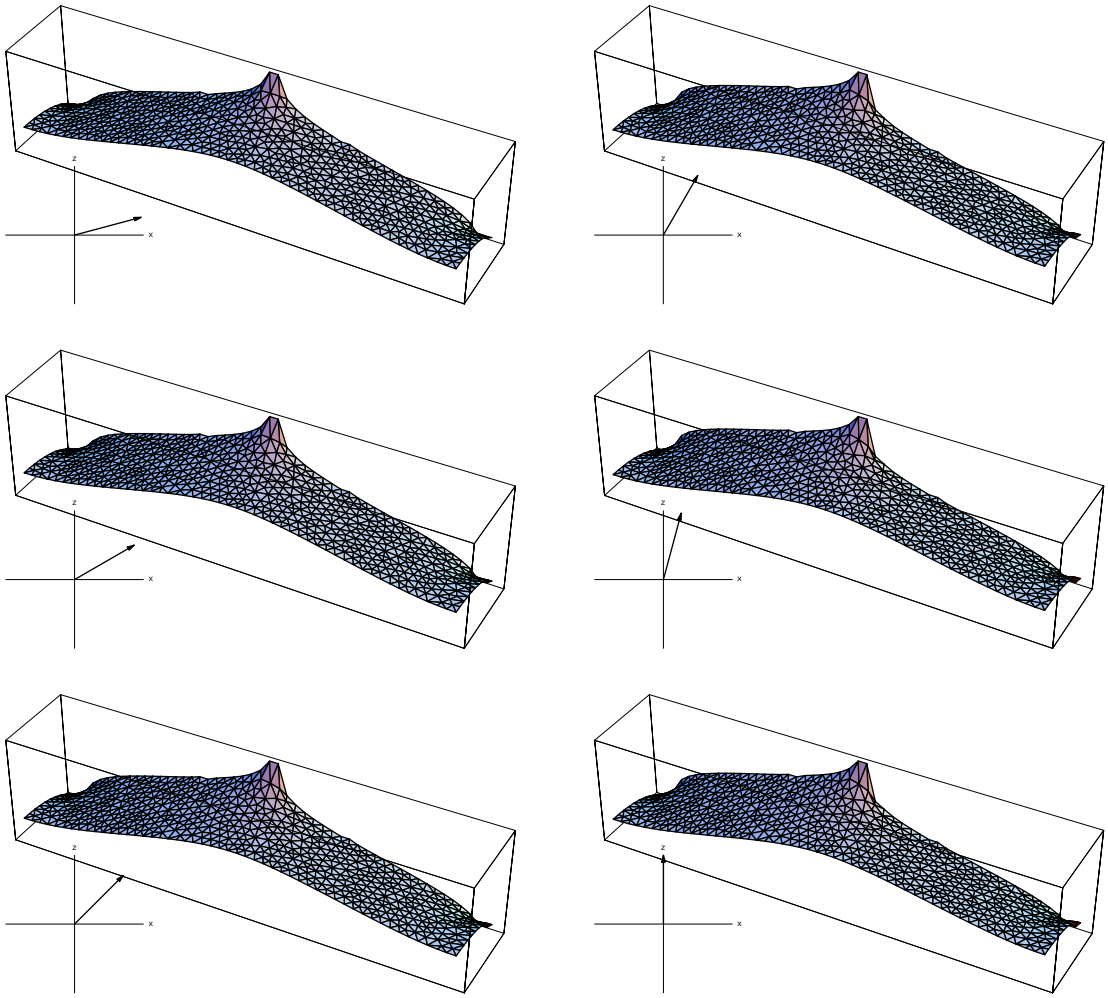

FIGURE 5. The potential distribution shown as a function of the orientation of the magnetic induction. The rotation is confined to the (x, z) plane. The device is biased as in figure 4. The asymmetry increases as the magnetic fields turns from the x to the y axis.

influence on the performance of a device with strong carrier confinement like trench-Hall devices. The speed of computation achieved by the utilization of two-dimensional finite-element discretization makes it a valuable tool for the designer to perform searches in parameter spaces.

REFERENCES

[1] R. Steiner Vanha, F. Kroener, T. Olbrich, R. Baresch, H. Baltes, "Trench Hall Devices", *IEEE J. Microelectromechanical Systems*, vol. 9 (2000), pp. 82–87.

[2] R. Steiner, C. Maier, M. Mayer, S. Bellekom, H. Baltes, "Influence of Mechanical Stress of the Offset Voltage of Hall Devices Operated with Spinning Current Method", *IEEE J. Microelectromechanical Systems*, vol. 8 (1999), pp. 466–472.

[3] A. Nathan, H. Baltes, W. Allegretto, "Review of physical models for numerical simulation of semiconductor microsensors", *IEEE Trans. on Compuer-Aided Design of Integrated Circuits and Systems*, vol. 9 (1990), pp. 1198–1208.

[4] C. S. Smith, "Piezoresistance effect in germanium and silicon", *Physical Review*, vol. 34 (1951), 129–132.

[5] B. Hälg, "Piezo-Hall coefficients of *n*-type silicon", *J. Applied Physics*, vol. 64 (1988), 276–282.

[6] M. Emmenegger, S. Taschini, J. G. Korvink, H. Baltes, "Simulation of a thermomechanically actuated gas sensor", *Proc. IEEE MEMS*, Heidelberg: 1998, pp. 184–189.